Rev.Adv.Mater.Sci. 22(2009) 60-66

HYDROTHERMAL SYNTHESIS OF Co_3O_4 NANO-OCTAHEDRA AND THEIR MAGNETIC PROPERTIES

Ana Fernández-Osorio[1], América Vázquez-Olmos[2], Roberto Sato-Berru[2] and Roberto Escudero[3]

[1]Facultad de Estudios Superiores Cuautitlán, Universidad Nacional Autónoma de México, A. P. 25, 54740 Edo de Méx., México
[2]Centro de Ciencias Aplicadas y Desarrollo Tecnológico, Universidad Nacional Autónoma de México, A. P. 70-186, 04510, México D.F. México
[3]Instituto de Investigaciones en Materiales, Universidad Nacional Autónoma de México. A.P.70-360, 04510, México D.F. México

Received: June 04, 2009

Abstract. Highly uniform cobalt oxide (Co_3O_4) nano-octahedra with mean edge length about 16.4±3.1 nm have been prepared using a hydrothermal method. X-ray diffraction pattern shows the normal spinel structure with formula $Co^{2+}(Co^{3+})_2O_4$ as the only crystallographic phase. The Co_3O_4 nanoparticles were characterized by UV-Vis and Raman spectroscopies and its morphology was determined by scanning and high resolution transmission electron microscopies. Magnetic properties of Co_3O_4 nano-octahedra were determined with a MPMS SQUID magnetometer. The blocking temperature (T_b) at 8K and a slight hysteresis loop indicating a ferrimagnetic behavior were observed. The magnetic response could be explained by uncompensated surface spins of the Co_3O_4 nanoparticles.

1. INTRODUCTION

Cobalt oxide (Co_3O_4) is a promising material for use as a gas sensor and catalyst in hydrocracking processes of crude fuels, pigment for glasses and ceramic. [1-5]. Highly dispersed nanostructured spinel cobalt oxide is expected to display better performance in the above mentioned application aspects. Specific morphologies and crystallographic phases of nanostructures materials are responsible for their optical, magnetic and electric properties [6].

Co_3O_4 belongs to the normal spinel structure, which is based on a cubic close packing array of oxide ions in which Co(II) ions occupy the tetrahedral 8a sites and Co(III) ions ocuppy the octahedral 16d sites [7]. Synthesis of cobalt oxide nanoparticles have been obtained by different methods as solvothermal, mechanochemical, reduction–oxidation, sol-gel and polymer combustion, generating different morphologies like nanotubes, nanorods, nanocubes, and spherical particles [8-19].

Increasing interest has been generated with antiferromagnetic nanoparticles since the discovery of their potentials for quantum tunneling [20,21] and their applications in spin-valve systems [22]. In bulk crystalline form, Co_3O_4 exhibits antiferromagnetism with Néel temperature of about T_N = 33K [23].

Early studies by Néel suggested that nanoparticles of antiferromagnetic materials should exhibit superparamagnetic behavior or a weak ferromagnetism, which may be ascribed to the reduced coordination of the surface spins, leading to important changes in the magnetic order.

Corresponding author: Ana Fernandez-Osorio, e-mail: ana8485@servidor.unam.mx

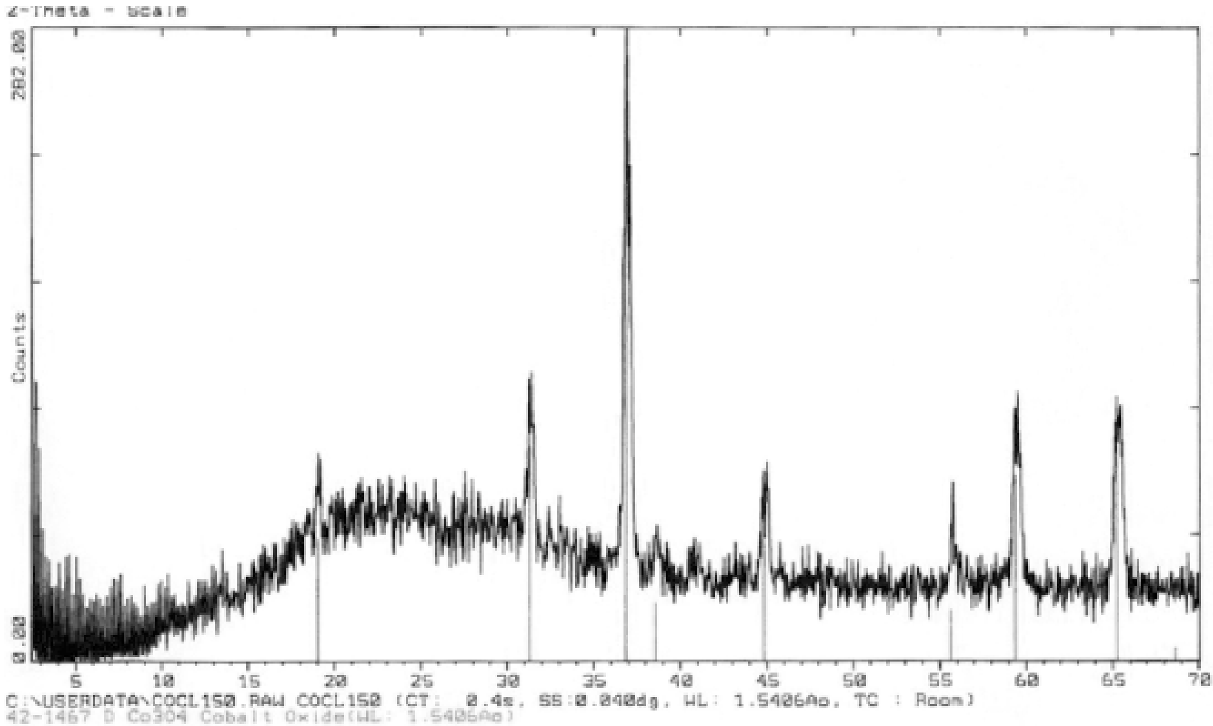

Fig. 1. XRD pattern of Co_3O_4 nanoparticles. All peaks can be indexed to Co_3O_4 cobaltite, with structure given by JCPDS No.421467.

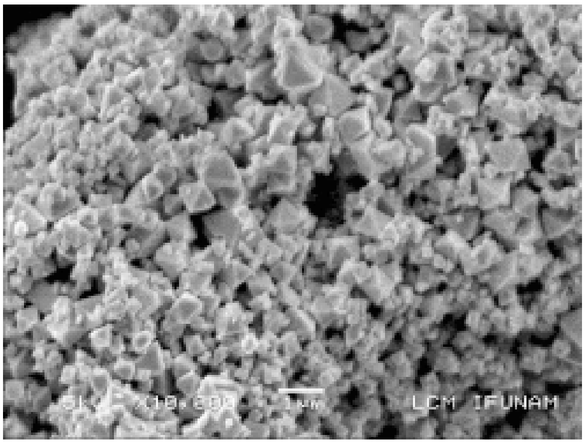

Fig. 2. SEM micrograph of Co_3O_4 nanoparticles. Note the spinel octahedral morphology.

Makhlouf [24] reported magnetization and magnetic relaxation measurements in Co_3O_4 particles with sizes about 20 nm, he observed a narrow cusp at about 25K in zero field-cooling (ZFC) magnetization and irreversibility in the field-cooling mode (FC). Both FC and ZFC modes bifurcate at lower temperatures. Above 60K magnetization temperature measurements, *M-T* obey Curie-Weiss law with negative Weiss temperature, θ at about 85K.

In this work, we present a facile synthesis method, in mild reaction conditions to obtain Co_3O_4 nano-octahedra with average crystallite size of 16.4±3.1 nm, and their structural and magnetic study

2. EXPERIMENTAL

2.1 Synthesis

In a typical synthesis, an aqueous solution of 0.4M $CoCl_2 \times 6H_2O$ (Aldrich 99%) was prepared adding drop to drop 0.5 ml of 0.5 M ammonium hydroxide up to obtain a pink precipitate (pH 8±0.5) of $Co(OH)_2$ according to following reaction:

$$CoCl_2 + NH_4OH \xrightarrow{RT} Co(OH)_2 + NH_4^+ + Cl.$$

The precipitate was washed with distilled water to remove Cl^- and NH_4^+ ions, and the final product was dried at room temperature and then, calcined in air at 150 °C for 2 h as follows:

$$3\,Co(OH)_2 + 1/2\,O_2 \xrightarrow{150\ °C,\ 2\ hrs} Co_3O_4 + 3\,OH_2.$$

2.2. Characterization Techniques

X-ray diffraction pattern was obtained at room temperature with Cu K_α radiation (λ = 1.5406 Å) be-

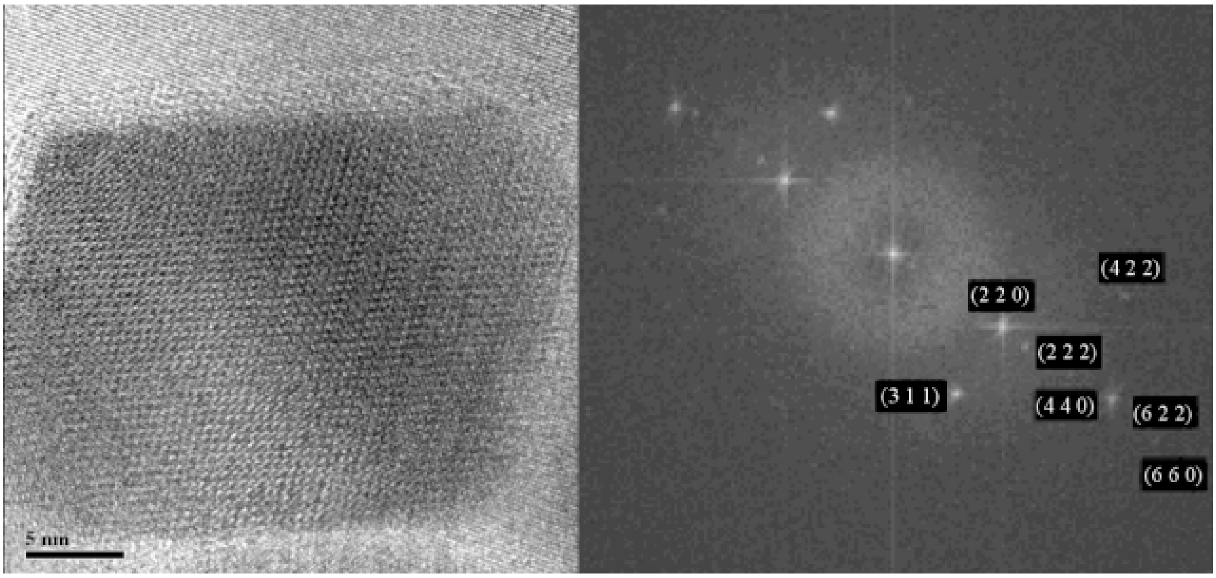

Fig. 3. HR-TEM micrograph of nanocrystalline Co_3O_4 and its corresponding electron diffraction pattern.

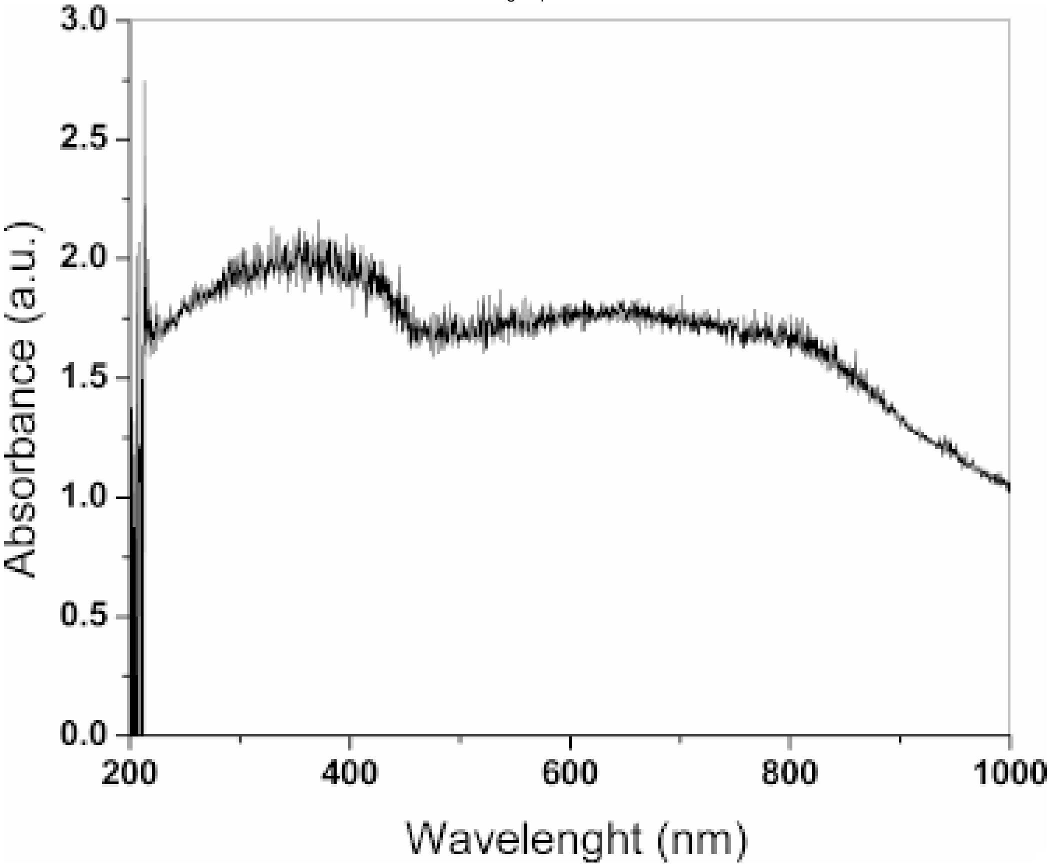

Fig. 4. UV-visible electronic absorption spectrum of Co_3O4 Nps.

tween 2.5° and 70° with a 2θ step of 0.02° for 0.8 s per point, using a D5000 Siemens diffractometer. UV-Vis electronic absorption spectrum was measured in diffuse reflectance mode in the 200–1200 nm wavelength range with an Ocean-optics HR4000 spectrometer. Raman spectrum was obtained from 200 to 900 cm^{-1} with a Nicolet Almega XR dispersive Raman spectrometer, using a scan time of 25 s and resolution of ~4 cm^{-1}. An Nd:YVO_4 532-nm laser was used for excitation and the inci-

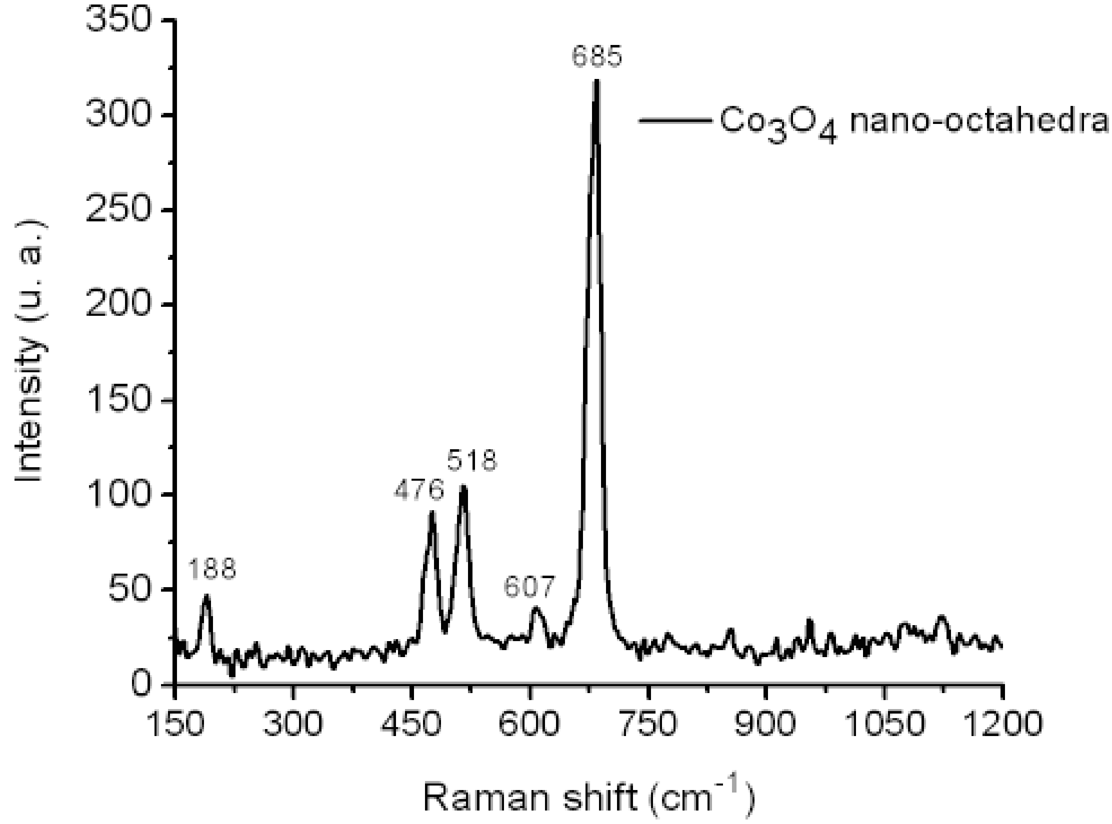

Fig. 5. Raman spectrum of Co_3O_4 nano-octahedral.

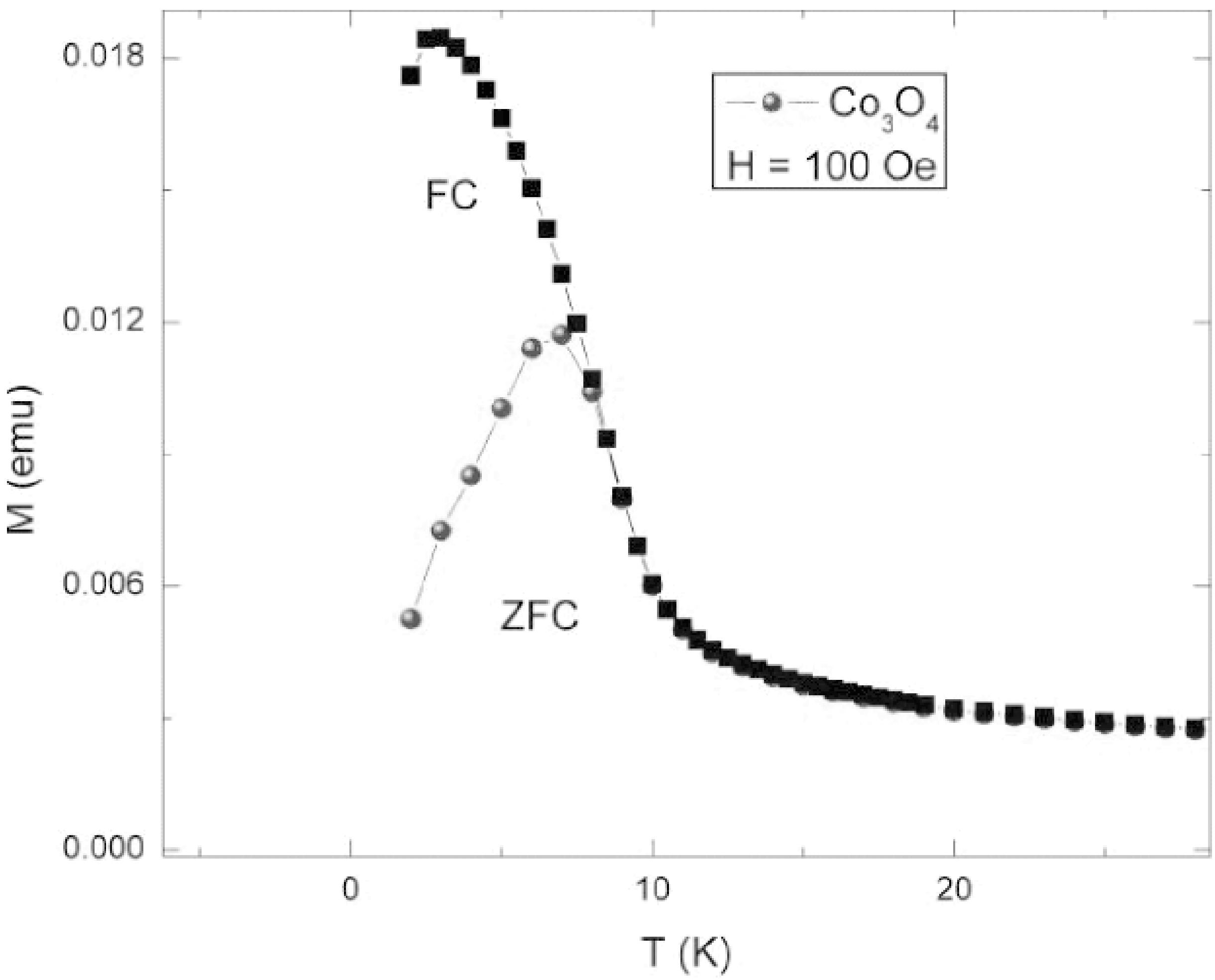

Fig. 6. Temperature dependence of FC and ZFC magnetization for Co_3O_4 nanoparticles.

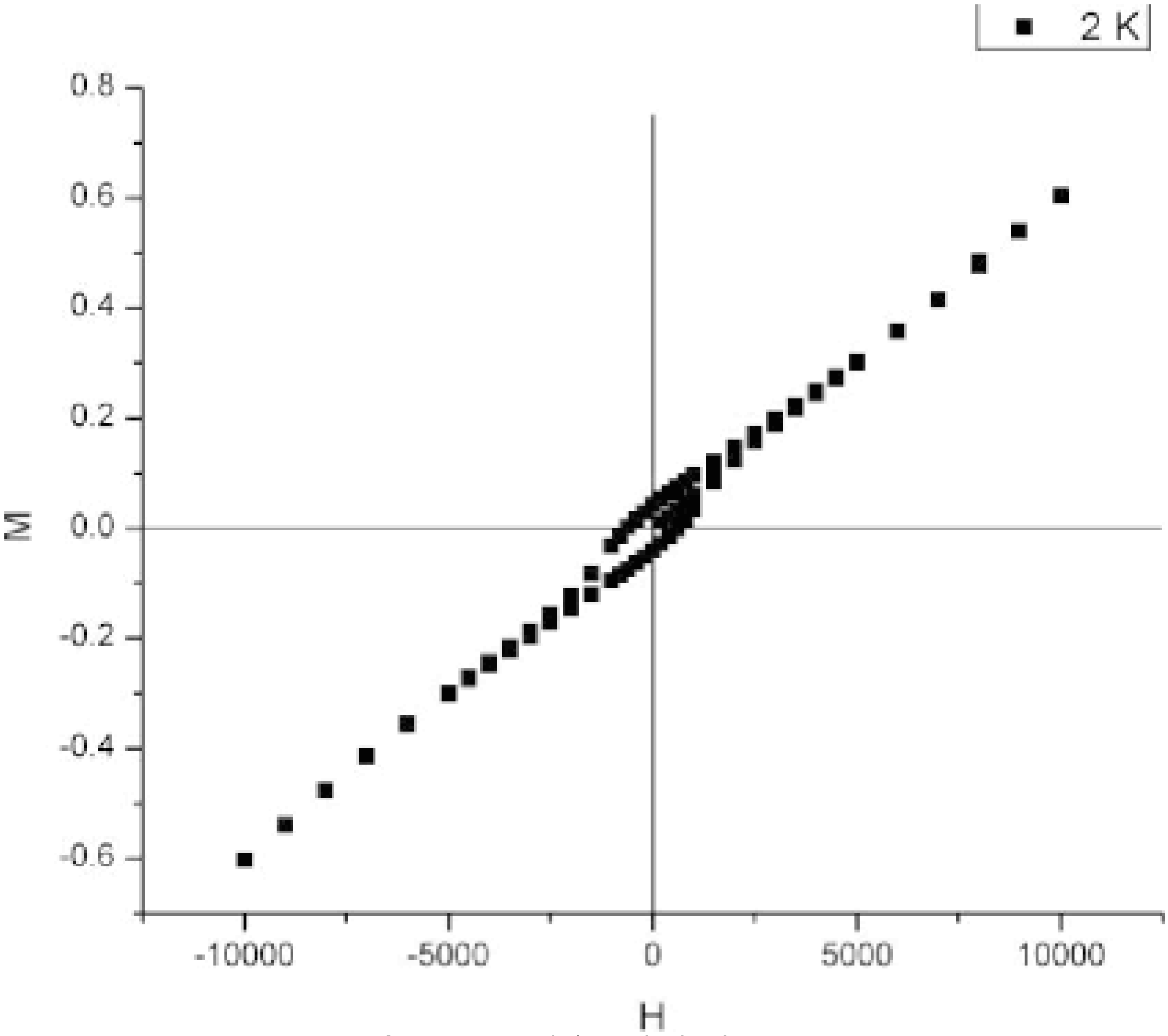

Fig. 7. Hysteresis loop obtained at 2K.

dent power on the sample was ~10 mW. High-resolution transmission electron micrographs (HR-TEM) were obtained in a JEOL 2010 FASTEM analytical microscope operating at 200 kV, by deposition of Co_3O_4 powder dispersed in methanol onto a 200-mesh Cu grid coated with carbon layer. Scanning electron micrographs (SEM) were obtained in a JEOL JSM5900 LV microscope by direct immersion of a grid into Co_3O_4 powder, without the use of any solvent. Magnetic studies were performed on a MPMS SQUID Quantum Design Magnetometer on powdered sample of Co_3O_4 nano-octahedra. The temperature was varied between 2 and 300K according to a zero field cooling (ZFC)/field cooling (FC) procedure at 100 Oe, and the hysteresis loop was obtained at 2K, in a magnetic field of up to ± 3T.

3. RESULTS AND DISCUSSION

The X-ray powder diffraction pattern of the nanocrystalline product is showed in Fig. 1. All diffraction peaks can be perfectly indexed to cobalt oxide Co_3O_4 spinel structure (JCPDS 42-1467) with a unit symmetry described by the space group Fd3m and lattice parameter a = 8.083 Å. The XRD pattern reveals the high purity of the sample.

To determine the average crystallite size (16.4±3.1 nm) we used the classical Scherrer equation over all reflections. The Co_3O_4 nano-crystals morphology was examined by SEM. Fig. 2 shows the formation of homogeneous nano-octahedra.

The HR-TEM micrograph (Fig. 3) shows an isolated Co_3O_4 nanocrystallite with dimensions of about 20.5 nm. The interplanar distances determined from their corresponding electron diffraction patterns confirm that the nanocrystals are composed of Co_3O_4.

With the aim of to study the optical response of the Co_3O_4 nano-octahedra, UV-Visible electronic absorption spectroscopy using diffuse reflectance technique (DRS) was obtained. Fig. 4 shows a typical absorption spectrum of Co_3O_4 nanoparticles where two wide absorption bands are observed. The first band from 250 to 450 nm involves the charge transfer transitions $O^{2-} \rightarrow Co^{2+}$ and $O^{2-} \rightarrow Co^{3+}$ and Co(III) in an octahedral site: $^1A_{1g} \rightarrow {}^1T_{2g}$. The second band centered about 650 nm is assigned to Co(III) in an octahedral site: $^1T_{1g} \leftarrow {}^1A_{1g}$ and Co(II) in a tetrahedral site: $^4T_1 \leftarrow {}^4A_2$ [25].

Furthermore, it is well known that Raman spectroscopy is a nondestructive technique which in the last years has been extensively used in nanostructure characterization. Fig. 5 shows the Raman spectrum of the nanocrystalline Co_3O_4, five active Raman modes characteristic of this cobalt oxides are evident at 188, 476, 518, 607, and 685 cm^{-1}, in agreement with those reported by Hadjiev et al. [26].

3.2 Magnetic measurements

Magnetic *M-T* measurements were performed at temperatures from 2 to 300K under a 100 Oe field. Fig. 6 shows the *M-T* curves of both FC and ZFC for the Co_3O_4 nano-ctahedra sample. T_N could not be observed at around 33K; however, the FC and ZFC curves were strongly bifurcated at 8K. This bifurcation temperature of FC and ZFC was defined as the blocking T_b temperature. These particles could be considered to form a single domain ordered antiferromagnetically, below T_N = 33K.

Magnetization far above T_b presents a paramagnetic behavior, whereas near above T_b, a superparamagnetic response was observed. The hysteresis curve at a temperature of 2K is given in Fig. 7. Coercivity was observed at 1200 Oe.

Below T_b, a slight hysteresis loop appears indicating a ferromagnetic behavior. This magnetic response could be explained by uncompensated surface spins of the Co_3O_4 nanoparticles. Ichiyanagi et al. [27] reported similar magnetic behavior on Co_3O_4 nanoparticles with an average size of between 3.1 and 9.2 nm.

4. CONCLUSIONS

Co_3O_4 nano-octahedra in a single spinel phase were obtained by a facile hydrothermal method at mild reaction conditions. A weak ferrimagnetism is observed at temperatures below 8K due to uncompensated surface spins behaving superparamagnetically, the total magnetic spins became easy to order. At high magnetic field, *M-T* follows a Curie-Weiss law without any irreversibility.

ACKNOWLEDGMENTS

The authors gratefully acknowledge the support from F. Silvar and DGAPA project IN106007.

REFERENCES

[1] L. D. Kadam and P. S. Patil // *Mater. Chem. Phys.* **68** (2001) 225.
[2] J. Wollenstein, M. Burgmair, G. Plescher, T. Sulima, J. Hildebrand, H. Botner and I. Eisele // *Sens. Actuators B* **93** (2003) 442.
[3] T. Kobayashi and M. Ando // *Electrochemistry* **69** (2001) 872.
[4] K. B. Zhou, X. Wang, X. M. Sun, Q. Peng and Y. D. Lee // *J. Catal.* **229** (2005) 206.
[5] S. Noguchi and M. Mizuhashi // *Thin Solid Films* **77** (1981) 99.
[6] G. D. Mahan, R. Gupta, Q. Xiong, C.K. Adu and P.C. Eklund // *Phys. Rev. B* **68** (2003) 73402.
[7] H. O´ Neill and A. Navrotsky // *Am. Mineral.* **68** (1983)181.
[8] N. Koshizaki, A. Narazaki and T. Sasaki // *Scripta Mater.* **44** (2001) 1925.
[9] J. Jiu, Y. Ge, X. Li and L. Nie // *Mat. Lett.* **54** (2002) 260.
[10] Q. Yuanchun, Z. Yanbao and W. Zhishen // *Mater. Chem. Phys.* **110** (2008) 457.
[11] Y. Ni, X. Ge, Z. Zhang, H. Liu, Z. Zhu and Q. Ye // *Mater. Res. Bull.* **36** (2001) 2383.
[12] H. Yang, Y. Hu, X. Zhang and G. Qiu // *Mat. Lett.* **58** (2004) 387.
[13] T. He, D. Chen, X. Jiao, Y. Xu and Y. Gu // *Langmuir* **20** (2004) 8404.
[14] X. Liu, G. Qiu and X. Li // *Nanotechnology* **16** (2005) 3035.
[15] X. Tang, J. Li and J. Hao // *Mater. Res. Bull.* **43** (2008) 21912.
[16] S. Lian, E. Wang, L. Gao and L. Xu // *Mat. Lett.* **61** (2007) 3893.
[17] R. Xu and H. Zeng // *J. Phys.Chem. B* **107** (2003) 926.
[18] R. Wang, C. Liu, H. Zhang and C. Chen // *Appl. Phys. Lett.* **85** (2004) 2080.
[19] Y. Liu, G. Wang, C. Xu and W. Wang // *Chem. Commun.* **14** (2002) 1486.

[20] M. M. Ibrahim, S. Darwish and M. Sehera // *Phys. Rev. B* **51** (1995) 2955.

[21] S. Hider, D. Awschalom, T. Douglas, S. Mann and M. Chaparla // *Science* **268** (1995) 77.

[22] I. Lopes, N. E. Hassan, H. Guerva, G. Wallez and A. Davidson // *Chem. Mat.* **18** (2006) 5826.

[23] W. L. Roth // *J. Phys.Chem. Solids* **25** (1964) 1.

[24] S. A. Makhlouf // *J. Magn. Magn. Mater.* **246** (2002) 184.

[25] G. A. Leon, G. L. Bezemer, J.A. Bergwerff and M.Verslujs-Helder // *J. Catal.* **242** (2006) 287.

[26] V. G. Hadjiev, M. N. Iliev and I. V. Vergilov // *J. Phys. C: Solid State Phys.* **21** (1988) L199.

[27] Y. Ichinagi and S. Yamada // *Polyhedron* **24** (2005) 2813.